

Part 5

METEORS, METEORITES

AND DUST

The origin and evolution of stony meteorites

William F. Bottke¹, D. Durda¹, D. Nesvorný¹, R. Jedicke²,
A. Morbidelli³, D. Vokrouhlický⁴, and H. Levison¹

¹Southwest Research Institute, 1050 Walnut St., Suite 400, Boulder, CO 80302, USA
W. F. Bottke's email: bottke@boulder.swri.edu

²Institute for Astronomy, University of Hawaii, Honolulu, Hawaii 96822

³Obs. de la Côte d'Azur, B.P. 4229, 06034 Nice Cedex 4, France

⁴Institute of Astronomy, Charles University, V Holešovičkách 2, 180 00 Prague

Abstract. The origin of stony meteorites landing on Earth today is directly linked to the history of the main belt, which evolved both through collisional evolution and dynamical evolution/depletion. In this paper, we focus our attention on the main belt dynamical evolution scenario discussed in Petit *et al.* (2001). According to Petit *et al.*, during the planet formation epoch, the primordial main belt contained several Earth masses of material, enough to allow the asteroids to accrete on relatively short timescales.

After a few My, the accretion of planetary embryos in the main belt zone dynamically stirred the remaining planetesimals to high enough velocities to initiate fragmentation. After a short interval, perhaps as long as 10 My, the primordial main belt was dynamically depleted of > 99% of its material via the combined perturbations of the planetary embryos and a newly-formed Jupiter. The small percentage of objects that survived in the main belt zone became the asteroid belt. It has been shown that the wavy-shaped size-frequency distribution of the main belt is a "fossil" left over from this violent period (Bottke *et al.* 2004).

Using a collisional/dynamical model of this scenario, we tracked the evolution of stony meteoroids produced by catastrophic disruption events over the last several Gy. We show that most stony meteoroids are a byproduct of a collisional cascade derived from large and ancient asteroid families or smaller, more recent breakup events. The meteoroids are then delivered to Earth by drifting in semimajor axis via Yarkovsky thermal drag forces until they reach a resonance powerful enough to place them on an Earth-crossing orbit.

Keywords. Minor planets, asteroids; collisional physics, impact processes, origin, solar system

1. Introduction

Meteorites are hand-samples of asteroids (and possibly comets) that have survived passage through our atmosphere to reach the Earth's surface. Properly analyzed, the bulk composition, mineralogy, and petrology of meteorites can be used to constrain planet formation processes as well as the evolution of the solar nebula. For example, by identifying where meteorites with different chemical and isotopic signatures originated, we may be able to deduce the compositional and thermal gradients that existed in the solar nebula (e.g., Burbine *et al.* 2002).

One of the most challenging aspects of this problem is placing our meteorite samples into the appropriate geologic context. At present, we have limited information on which meteorites go with which parent bodies (or their immediate precursors). Determining the linkages between meteorites and their parent bodies is a critical goal of asteroid and meteorite studies.

Our first task is to identify the source regions for those meteorites landing on Earth today. Before a meteorite can reach Earth, it must first become part of the Earth-crossing

object (ECO) population (perihelion distance $q \leq 1.017$ AU and aphelion distances $Q \geq 0.983$ AU). Bottke *et al.* (2000; 2002a) showed that nearly all of the observed ECOs (mainly diameter $D > 1$ km objects) originated in the main belt. Because most meteorites have physical properties similar to the observed main belt asteroids, and because meteoroids must follow the same dynamical pathways as km-sized ECOs (and near-Earth asteroids, or NEOs; $q \leq 1.3$ AU and $Q \geq 0.983$ AU) once they reach planet-crossing orbits, we infer that the majority of meteoroids reaching Earth are from the main belt (e.g., Vokrouhlický & Farinella 2000).

Our next task is to determine how meteoroids, the meter-sized precursors of the meteorites, are delivered to Earth. Numerical simulations have shown that meteorites travel from the main belt to Earth through a two-step process.

In the first step, main belt asteroids collide with one another at high velocities (~ 5 km s⁻¹; Bottke *et al.* 1994) and undergo fragmentation (see Asphaug *et al.* 2002 and Holsapple *et al.* 2002 for recent reviews). The orbits, spin states, shapes, and internal structures of the surviving bodies are determined from the kinetic energy and specific nature of the impact. The largest disruption events occurring in main belt over the last several Gy produced the observed asteroid families (e.g., Zappalá *et al.* 2002). The typical ejection velocities produced by these fragmentation events are $\lesssim 100$ m s⁻¹ (Bottke *et al.* 2001; Michel *et al.* 2001; 2002; 2003); in most cases, this leaves the ejecta relatively close to the impact site (i.e., within a few 0.01 AU).

In the second step, fragments with diameter $0.0001 < D < 20$ km undergo slow but steady dynamical evolution via the Yarkovsky effect, a thermal radiation force that causes small objects to undergo semimajor axis drift as a function of their spin, orbit, and material properties. As described in the chapter by Vokrouhlický *et al.* (2004; this book), the drift rate for meter-size stones in the main belt is $\pm(0.01\text{-}0.001)$ AU My⁻¹, while the drift rate for iron meteoroids is ~ 10 times slower.

This process drives some of these objects into powerful resonances produced by the gravitational perturbations of the planets (e.g., the 3:1, ν_6 resonances). Numerical studies show that test objects placed in such resonance have their eccentricities pumped up to planet-crossing orbits (e.g., Wisdom 1983). Once on planet-crossing orbits, meteoroids have their dynamical evolution dominated both by resonances and gravitational close encounters with the planets. A small fraction of these bodies go on to strike the Earth ($\sim 1\%$; Gladman *et al.* 1997; Morbidelli & Gladman 1998), though most impact the Sun or are ejected from the inner solar system via a close encounter with Jupiter (Farinella *et al.* 1992; Gladman *et al.* 1997).

The missing component in this description is collisional evolution, namely the length of time meteoroids survive against collisional disruption. If collision disruption timescales are short, the immediate precursors of nearly all meteorites must be in the NEO/ECO populations, while if they are long, the immediate precursors are likely to be main belt asteroids. An important clue used to determine the immediate source region of most meteoroids is the cosmic-ray exposure (CRE) ages of meteorites. CRE ages measure the time interval spent in space between the meteoroid's formation as a $D < 3$ m body (following removal from a shielded location within a larger object) and its arrival at Earth (e.g., Morbidelli and Gladman 1998). The CRE ages of most stony meteorites are between $\sim 10\text{-}100$ My, while iron meteorites have CRE ages between $\sim 0.1\text{-}1.0$ Gy (Caffee *et al.* 1988; Marti & Graf 1992; Eugster 2003). Because these timescales are longer than the average dynamical lifetime of near-Earth asteroids (~ 4 My; Bottke *et al.* 2002a), we infer that many meteoroids, particularly iron meteoroids, had to obtain considerable damage from cosmic rays while drifting in the main belt as a meter-sized body. Thus, it is likely that most meteoroids originated in the main belt.

Given that there are more than 20,000 meteorites in our existing collection (Grady 2000), and that the meteoroid delivery scenario described above allows nearly any main belt asteroid to produce meteoroids, one would expect the Earth to be on the receiving end of samples from thousands upon thousands of distinct parent bodies. Tests of these samples, however, suggests the opposite; our meteorite collection could represent as few as ~ 100 different asteroid parent bodies: ~ 27 chondritic, ~ 2 primitive achondritic, ~ 6 differentiated achondritic, ~ 4 stony-iron, ~ 10 iron groups, and ~ 50 ungrouped irons (Meibom & Clark 1999; Keil 2000; 2002; Burbine *et al.* 2002). If we ignore the stony-iron, iron, and differentiated meteorites for the moment, this number is reduced to ~ 30 objects. This value seems surprisingly small when one considers the large number of main belt asteroids that should have disrupted over the last 4.6 Gy.

What are our models missing? As far as we can tell, our numerical simulations are doing a reasonable job of tracking the dynamical evolution of meteoroids throughout the inner solar system. Our treatment of collisional evolution among the meteoroid population, however, is less advanced. At present, we have yet to realistically track how meteoroids evolve via comminution over several Gy of solar system history. This is a difficult problem, partly because main belt collisional models need accurate starting conditions and constraints, but also because the outcome is strongly linked to the main belt's dynamical history. For example, the dynamical events occurring during the planet formation era (e.g., wandering planetary embryos, the formation of the Jovian planets) almost certainly influenced the main belt population observed today.

Thus, to correctly model meteoroid evolution, we need to be able to:

(i) determine how the main belt population collisionally and dynamically evolved over its history,

(ii) model the disruption of individual parent bodies within such a model,

(iii) track how the fragment size distribution of each parent body evolves with time,

(iv) determine how the meteoroid population derived from each parent body is affected by sources (e.g., new meteoroids produced by a 'collisional cascade' among the parent body's fragment size distribution) and sinks (e.g., dynamical loss mechanisms such as Yarkovsky effect/resonances; collisional disruption),

(v) determine how many meteoroids from each disrupted parent body would have reached Earth over a window starting ~ 0.1 Ma (i.e., the maximum terrestrial residence time of stony meteorites in the Antarctic; Bland *et al.* 1998).

At present, we are still struggling to accurately model these processes. Despite this, our group has made enough recent progress to show some interesting preliminary results in this brief paper. Our focus will be on the origin and evolution of the stony meteorites; we save a discussion of iron meteorites for future work. We start with a discussion of how the main belt may have dynamical evolved over solar system history.

2. Dynamical Evolution of the Main Belt

One of the most important constraints on planet formation processes is the apparent mass depletion of the main belt. During the planet formation epoch, the primordial main belt was believed to have contained several Earth masses of material, enough to allow the asteroids to accrete on relatively short timescales (e.g., Weidenschilling 1977; Wetherill 1989). The present-day main belt, however, only contains ~ 0.0005 Earth masses of

material (e.g., Britt *et al.* 2002). Though several scenarios have been proposed to explain this putative loss of mass (e.g., see review by Petit *et al.* 2002), the best available model at present is that described by Petit *et al.* (2001). We describe their results by dividing them into 3 distinct phases.

2.1. Phase 1: Dynamical Excitation of the Primordial Main Belt by Embryos

Planetesimals and planetary embryos accreted in the primordial main belt during the first few My of solar system history. According to planetary accretion models, runaway growth should have produced Moon- to Mars-size embryos throughout the inner solar system (< 4 AU) over a timescale of ~ 0.1 -1 My (Wetherill 1989; Wetherill & Stewart 1989; Weidenschilling & Davis 2001). Models describing the evolution of planetary embryos and planetesimals in the inner solar system have been investigated by several groups (e.g., Wetherill 1992; Agnor *et al.* 1998; Chambers & Wetherill 1998; 2001; Petit *et al.* 2001).

Once formed, planetary embryos in the inner solar system perturbed both themselves and the surviving planetesimals. This was modeled by Petit *et al.* (2001), who tracked the evolution of 56 embryos started on circular, slightly inclined orbits (0.1°) between 0.5 and 4 AU using the MERCURY integration package (Chambers & Migliorini 1997), and then created several simulations where the recorded masses, positions, and velocities of the embryos were used to gravitationally perturb test bodies initially placed on circular, zero inclination orbits. The test bodies were designed to represent asteroids in the primordial main belt that failed to accrete with various planetary embryos during runaway growth. The dynamical evolution of the test bodies were tracked using the numerical integrator SWIFT-RMVS3 (Levison & Duncan 1994), with perturbations of the planetary embryos included using techniques described by Petit *et al.* (1999).

Petit *et al.* (2001) found that after 1-2 My, planetesimal e, i values were already high enough to initiate fragmentation, while at 10 My, the e, i values of some test bodies were as high as ~ 0.6 and $\sim 40^\circ$, respectively. These perturbations cause collision velocities to steadily increase throughout Phase 1.

2.2. Phase 2: Dynamical Depletion of the Main Belt by Embryos and Jupiter/Saturn

In the core accretion model, planetary embryos were also forming near where Jupiter is found today (~ 5 AU). At some unknown time during Phase 1, these embryos merged and produced a ~ 2 -20 Earth mass core, where the core's large size may have been a byproduct of water ice condensation beyond the so-called "snowline" (Wuchterl *et al.* 2000; Inaba *et al.* 2003). Numerical modeling results suggest that once this core was massive enough to accrete gas from the solar nebula, Jupiter obtained its full size within ~ 1 My (e.g., Pollack *et al.* 1996). It is believed that Jupiter (and presumably Saturn) formed $\lesssim 10$ My after the formation of the first solids (Pollack *et al.* 1996; Guillot & Hueso 2003).

The introduction of Jupiter and Saturn into the solar system, which marks the beginning of Phase 2, had a dramatic effect on the dynamical structure of the primordial main belt (Fig. 1). To simulate this, Petit *et al.* (2001) injected Jupiter and Saturn, with their present-day masses and orbital elements, into the evolving system of embryos described in Phase 1 at 10 My. They found that gravitational perturbations from Jupiter and Saturn, when combined with the mutual gravitational perturbations of the embryos, dynamically excited those bodies residing in the main belt. In most simulations, the embryos achieved high enough e, i values to push themselves out of the main belt. Eventually, as the embryos collided and merged, a system of terrestrial planets was formed.

Fig. 1 shows several snapshots of the evolution of the embryos in the Petit *et al.* simulations. In the end, they produced two terrestrial planets, one with 1.3 Earth masses ($a = 0.68$ AU, $e = 0.15$, and $i = 5^\circ$) and another with 0.48 Earth masses ($a = 1.5$ AU, $e = 0.03$, and $i = 23^\circ$). This result illustrates the success and failures of the current generation of late-stage planet formation models; it is possible to generate terrestrial planet systems reminiscent of our Solar System, but the planets are dynamically hotter than Earth and Venus. Despite these limitations, however, the terrestrial planets produced by Petit *et al.* (2001) are similar enough to our own system (e.g., no planet is crossing the main belt) that they can be used to investigate the evolution of the primordial main belt.

To determine what happened to the main belt after the formation of Jupiter, Petit *et al.* (2001) inserted 100 test bodies on circular, low inclination orbits between 1.0-2.0 AU and 1000 test bodies between 2.0-2.8 AU into the embryo/Jupiter/Saturn system described above (Fig. 1). The test bodies were tracked for 100 My, with their orbits modified by the combined perturbations of the embryos and Jupiter/Saturn. Fig. 1 shows the test bodies becoming highly excited, with most objects eliminated by striking the Sun or being thrown out of the inner solar system via a close encounter with Jupiter after a few My. For the 1000 bodies started between 2.0-2.8 AU, five survived to become embedded within the main belt zone. These results imply that the main belt may have dynamically lost $\gtrsim 99\%$ of its primordial material through dynamical excitation.

The end of Phase 2 is somewhat nebulous. We believe a good working definition is the time when the dynamically-excited population becomes depleted enough that it is no longer capable of producing a statistically significant number of disruptions in the main belt population. Using dynamical results from Morbidelli *et al.* (2001), we assume Phase 2 ends ~ 400 My after the end of accretion and the onset of fragmentation.

2.3. Phase 3: Collisional Evolution in a Depleted Main Belt

In Phase 3, the surviving main belt bodies were left in a dynamical state comparable to the current main belt population. Any loss of material in Phase 3 is produced by the Yarkovsky effect, which drives multi-km and smaller asteroids into mean motion and secular resonances capable of pumping their e values onto planet-crossing orbits (e.g., Bottke *et al.* 2000; 2002a), and comminution. Nearly all asteroids escaping the main belt become part of the NEO population, though their dynamical lifetime in the NEO region varies considerably (see chapter by Vokrouhlický *et al.*)

Though there much to like about the Petit *et al.* (2001) scenario, we caution that it does not yet include the effects of the putative Late Heavy Bombardment (LHB), an event ~ 3.9 Gy ago where the inner solar system was ravaged by numerous impactors (e.g., Hartmann *et al.* 2000). We refer the reader to recent work by A. Morbidelli, K. Tsiganis, R. Gomes, and H. Levison (e.g., Gomes *et al.* 2004; Tsiganis *et al.* 2004) for additional details on the nature of the LHB.

Using the Petit *et al.* (2001) dynamical evolution scenario, we are now ready to model the collisional evolution in the main belt over solar system history. Our code and results are described below.

3. Collisional and Dynamical Depletion Evolution Model (CoDDEM)

To model the evolution of the main belt as completely as possible, we integrated the dynamical results described above with a self-consistent 1-D collisional evolution code (Bottke *et al.* 2004a,b). The essentials of this code, called CoDDEM (for collisional and dynamical depletion model), are briefly described below.

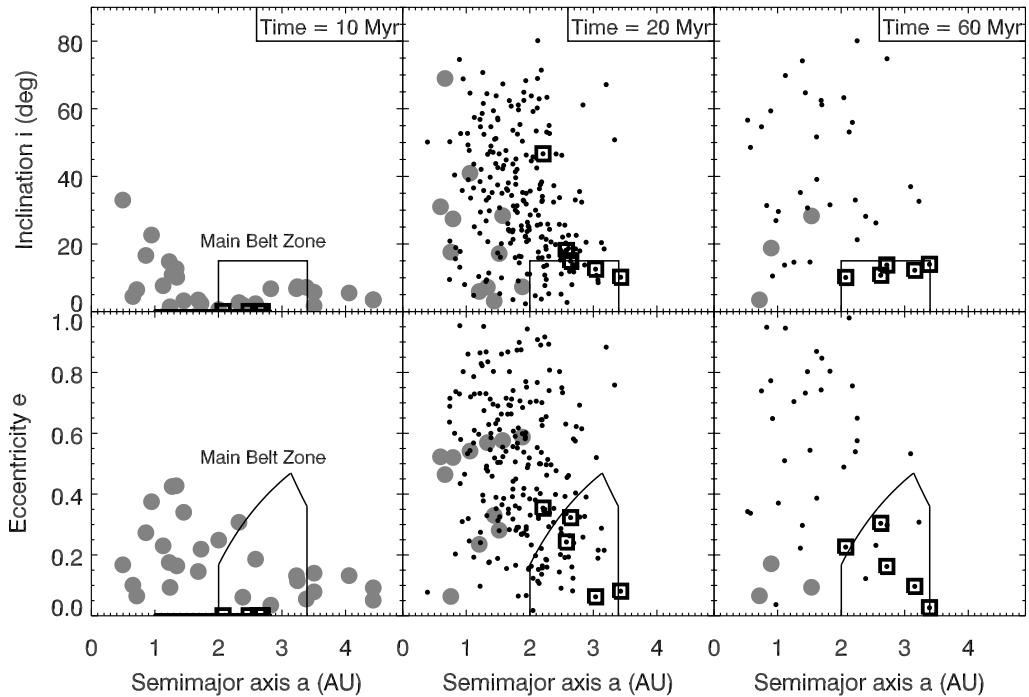


Figure 1. Three snapshots from a representative run in Petit *et al.* (2001), where the dynamical evolution of test bodies and planetary embryos were tracked for more than 100 Myr just after the formation of Jupiter (see Bottke *et al.* 2004b). The grey dots are planetary embryos, while the black dots are planetesimals. The black squares are centered on the 5 test bodies that will ultimately be trapped in the main belt zone. At $t = 20$ Myr, we see that nearly all of the test bodies have been pushed out of the main belt onto high e, i orbits. Perturbations from Jupiter have also eliminated or forced the merger of many embryos. By $t = 60$ Myr, the terrestrial planet system is nearly complete, with only a small remnant population left behind in the main belt zone. This system will eventually produce two terrestrial planets (see text).

We run CoDDEM by entering an initial main belt size-frequency distribution where the population (N) has been binned between $0.001 \text{ km} < D < 1000 \text{ km}$ in logarithmic intervals $d\text{Log}D = 0.1$. The particles in the bins are assumed to be spherical and are set to a bulk density of 2.7 g cm^{-3} (Britt *et al.* 2002; see Bottke *et al.* 2004a for details). CoDDEM then computes the time rate of change in the differential population N per unit volume of space over a size range between diameter D and $D + dD$ (Dohnanyi 1969; Williams & Wetherill 1994):

$$\frac{\partial N}{\partial t}(D, t) = -I_{\text{DISRUPT}} + I_{\text{FRAG}} - I_{\text{DYN}}. \quad (3.1)$$

All these terms are defined below.

Here I_{DISRUPT} is the net number of bodies that leave the bin between D and $D + dD$ per unit time from catastrophic disruption. The collisional lifetime of a body is computed using standard methods (e.g., Öpik 1951; Wetherill 1967; Greenberg 1982; Farinella & Davis 1992; Bottke & Greenberg 1993), where the “intrinsic” collision probabilities and impact velocities V_{imp} between the target body and background population are computed

directly from Phases 1-3 of the dynamical simulations described in Petit *et al.* (2001). For details, see Bottke *et al.* (2004b).

The projectile capable of disrupting D_{target} is defined as (d_{disrupt}):

$$d_{\text{disrupt}} = (2Q_{\text{D}}^*/V_{\text{imp}}^2)^{1/3} D_{\text{target}} \quad (3.2)$$

Q_{D}^* is defined as the critical impact specific energy; the energy per unit target mass needed to disrupt the target and send 50% of its mass away at escape velocity. In CoDDEM, we assume that $D < 150$ km disruption events are barely-catastrophic (i.e., 50% of the target body's mass is ejected). This means we neglect both cratering events, which produce much less ejecta over time than barely-catastrophic disruption events (e.g., Dohnanyi 1969; Williams & Wetherill 1994) and highly-energetic catastrophic disruption events, which are unlikely to occur (e.g., Love & Ahrens 1997). For $D > 150$ km disruptions, we assume they are super-catastrophic (i.e., more than 50% of the mass is ejected). We base this on the observation that the largest bodies found in families formed by $D \gtrsim 150$ km disruption events frequently contain $< 50\%$ of the mass of the original parent body (e.g., Eos, Themis) (Tanga *et al.* 1999; Bottke *et al.* 2004a). More discussion of this issue is given below.

For the simulations described in this paper, we use the Q_{D}^* function defined for basaltic targets described by the hydrocode runs of Benz & Asphaug (1994). This selection was corroborated by Bottke *et al.* (2004a), who used a CoDDEM-like code to show that Q_{D}^* functions similar to those described by Benz & Asphaug (1994) provide main belt collisional evolution results that are consistent with the available constraints (see below).

To remove disrupted bodies from our size-frequency distribution, we treated breakup events as Poisson random events, with integer numbers of particles removed (or not removed) from a size bin within a timestep according to Poisson statistics (Press *et al.* 1989). This means that different seeds for the random number generator can produce different outcomes. For this reason, our CoDDEM results are treated in a statistical manner; to get a quantitative measure of how good a given set of input parameters reproduces observations, we perform numerous trials using different random seeds before comparing our results to observations.

We defined I_{FRAG} as the number of bodies entering a size interval per unit time that were produced by the fragmentation of larger bodies. To determine I_{FRAG} , and to keep things as simple as possible given our unknowns in this area, we assume the fragment size distribution (FSD) produced by each catastrophic disruption event was similar to those observed in asteroid families like Themis (super-catastrophic) or Flora (barely-catastrophic) (Tanga *et al.* 1999; see Bottke *et al.* 2004a for details of how we chose our FSD values). Themis-like FSDs were developed for $D > 150$ km disruption events. We assumed the largest remnant was 50% the diameter of the parent body, and the incremental power law index between the largest remnant and fragments 1/60th the diameter of the parent body was -3.5. Fragments smaller than 1/60th the diameter of the parent body follow a power law index of -2.0. Flora-style FSDs were developed for breakups among $D < 150$ km bodies. Here the diameter of the largest remnant is set to 80% the diameter of the parent body. We gave these FSDs incremental power law indices, from the large end to the small end, of -2.3, -4.0, and -2.0, with transition points at 1/3 and 1/40 the diameter of the parent body. Note that in both cases, we assume that some material is located below the smallest size used by CoDDEM ($D = 0.001$ km) in the form of small fragments or regolith. Accordingly, mass is roughly but not explicitly conserved.

We defined I_{DYN} to be the number of bodies lost via dynamical processes from the size interval per unit time. The loss mechanisms could be those described in Phase 2 above or

by the Yarkovsky effect/resonances. For the latter, we assumed a size-dependent removal rate for main belt asteroids in each size interval (e.g., Farinella & Vokrouhlický 1999). Given the uncertainties in choosing these values (e.g., unknown spin rates, thermal conductivities, interaction between Yarkovsky and the so-called YORP mechanism that can change the spin vectors of asteroids; see Rubincam 2000), we decided base our Yarkovsky removal rate function for $D > 1$ km bodies on numerical results described in Morbidelli and Vokrouhlický (2003). Morbidelli and Vokrouhlický (2003) imposed a steady state on the inner main belt population and tracked their removal via Yarkovsky effect and resonances. Their model included factors such as collisional disruption, collisional spin axis reorientation events, and the effects of YORP. Accordingly, our removal rates decrease from 0.03% per My for $D = 1$ km bodies to 0.008% per My for $D = 10$ km bodies. This trend was continued down to 0.005% per My for $D = 20$ km bodies and 0.0002% for $D = 30$ km bodies. Beyond this point, we assume nothing escapes the main belt.

For $D < 1$ km bodies, our removal rate model is uncertain, with little trustworthy numerical work done on this issue to date. For this reason, we kept things simple and assumed sub-km asteroids ($0.001 < D < 1$ km) are removed at the same rate as $D \sim 1$ km asteroids (0.03% per My). Our main justification for this loss rate is that it provides a surprisingly good match to shape of the NEO population (see below). Vokrouhlický and Farinella (2000), however, show there are asteroidal thermal conductivity values that allow bodies ranging from cm- to km-sized objects to travel approximately the same distance in semimajor axis before disrupting. Given our uncertainty about asteroidal thermal conductivity values for sub-km-sized bodies, we believe our loss rate estimates are as good an estimate as any other currently available.

To calibrate our Yarkovsky effect/resonance removal rate functions, we ran numerous CoDDEM simulations and compared our model NEO population to estimates of the observed population between $0.001 < D \lesssim 10$ km (Stokes *et al.* 2003; Stuart & Binzel 2004). We found the above parameters produced a model NEO population that was a good match with observations.

4. Model Constraints

We tested our CoDDEM model results against a wide range of main belt constraints. One important constraint was the wavy-shaped main belt size distribution. To determine its value, we converted the absolute magnitude H distribution of the main belt described by Jedicke *et al.* (2002), who combined observations of bright main belt asteroids with renormalized results taken from the Sloan Digital Sky Survey (Ivezić *et al.* 2001), into a size distribution. This was accomplished using the relationship $D(\text{km}) = \frac{1329}{\sqrt{p_v}} 10^{-H/5}$ (Fowler & Chilemi 1992), and a representative visual geometric albedo $p_v = 0.092$. This produces a main belt population with 1.36×10^6 , 680, and 220 asteroids for $D > 1$, 50 and 100 km, respectively. These results are consistent with estimates from IRAS/color-albedo data (e.g., Farinella & Davis 1992; Tedesco *et al.* 2002), main belt population estimates from the ISO spacecraft (Tedesco & Desert 2002), and numerical simulations (Morbidelli & Vokrouhlický 2003).

A second set of constraints was provided by asteroids families, particularly those that are too large to be dispersed by the Yarkovsky effect over the age of the solar system (Nesvorný & Bottke 2004; Nesvorný *et al.* 2004). Using hydrocode simulations (Durda *et al.* 2004) to estimate the amount of material in families located below the observational detection limit, we computed that ~ 20 families have been produced by the breakup of $D \gtrsim 100$ asteroids over the last ~ 3.5 Gy (Bottke *et al.* 2004a).

CoDDEM adopts the same constraint; we assume that the size distribution bins centered on $D = 123.5, 155.5, 195.7, 246.4, 310.2,$ and 390.5 km experienced 5, 5, 5, 1, 1, 1 breakups over the last 3.5 Gy, respectively.

A third constraint comes from studies of the cratering record on the lunar maria, which shows the NEO impact flux has been relatively constant over the last ~ 3 Gy (e.g., Grieve & Shoemaker 1994). This result implies the NEO population (and thus the main belt population) has been in a quasi-steady state over this time period.

Other constraints are described by Bottke *et al.* (2004a,b).

5. Initial Conditions and a Sample CoDDEM Run

The initial main belt population entered into CoDDEM is divided into two components that are tracked simultaneously: a small component of main belt asteroids that will survive the dynamical excitation event (DDE) described in Phase 2 (N_{rem}) and a much larger component that will be excited and ejected from the main belt during the Phase 2 DDE (N_{dep}). Thus, our initial population is $N = N_{\text{rem}} + N_{\text{dep}}$. We can use this procedure because we know in advance the dynamical fate of each population via the dynamics simulations described in Sec. 2. The two populations undergo comminution with themselves and with each other. At the end of Phase 2 (i.e., when $N_{\text{dep}} = 0$), CoDDEM tracks the collisional and dynamical evolution of N_{rem} alone for the remaining simulation time.

The size and shape of our initial size distribution was determined by running different initial populations through CoDDEM-like codes and then testing the results against the constraints described in Sec. 4 (Durda *et al.* 1998; Bottke *et al.* 2004a,b). The size distribution that provided the best fit for N_{rem} followed the observed main belt for $D > 200$ km bodies, an incremental power law index of -4.5 for $110 < D < 200$ km bodies, and an incremental power law index of -1.2 for $D < 110$ km bodies (Bottke *et al.* 2004b). The initial shape of the N_{dep} population is always the same as N_{rem} , but its size can be increased or decreased depending on when Jupiter reaches its full size (i.e., the length of Phase 1) (Bottke *et al.* 2004b). For the runs shown here, we set $N_{\text{dep}} = 200N_{\text{rem}}$ and we assumed that Jupiter reached its full size 4 My after the onset of main belt fragmentation.

An example of one successful CoDDEM run is shown in Fig. 2. The $t = 0$ My timestep shows our initial conditions. The $t = 3$ My timestep shows a bump developing near $D \sim 2\text{--}3$ km for both N_{rem} and N_{dep} ; this is a by-product of the “V”-shaped Q_{D}^* function (Campo Bagatin *et al.* 1994; Durda *et al.* 1998; Davis *et al.* 2002). Self-gravity among $D > 200$ m objects makes them increasingly difficult to disrupt. This produces an “over-abundance” of $D \sim 200$ m objects that induces a wave-like perturbation into the main belt size distribution. The $t = 30$ My timestep shows the N_{dep} population significantly depleted, with few members lasting beyond 100 My. Concurrently, impacts on N_{rem} from N_{dep} eventually produce a shape for its size distribution that approaches that of the observed main belt. [In this paper, when we say “observed main belt”, we are usually including the portion of the main belt size distribution that has been inferred from debiased observational data (Jedicke *et al.* 2002; see also Bottke *et al.* 2004a).] This explains how the NEO/ECO population (and the impact flux on the Moon) could have been in quasi-steady state for several Gy. A good fit to the main belt population (and to the population of asteroid families) is achieved at 4.6 Gy. Our results show a good match to the estimated NEO population between $0.001 < D < 10$ km. This is not a surprise given that our Yarkovsky effect/resonance removal function was selected for this purpose.

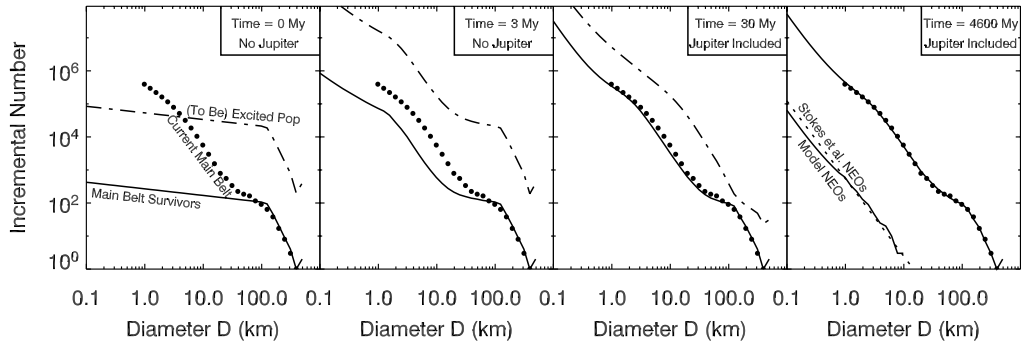


Figure 2. Four snapshots from a representative run where we track the collisional evolution of the main belt size distribution for 4.6 Gy. The starting population is divided into two components: the “main belt survivors”, who will be left behind in the main belt zone, and the “(To be) excited population”, who will be scattered out of the main belt via perturbations from embryos and Jupiter. Here the former population is 200 times smaller than the latter, with Jupiter entering the system at 4 My. The dots represent the observed main belt. The bump observed in most frames near $D \sim 2\text{--}3$ km is driven by the shape of the asteroid disruption scaling law. The 30 My timestep shows this population significantly depleted, with few members lasting beyond 100 My. A good fit to the main belt and NEO populations is achieved at 4600 My. Note that the NEO population from Stokes *et al.* (2003) was determined by fitting a line to the $D > 1$ km bodies; our model NEO population actually provides a better fit to the available $D < 1$ km NEO data than Stokes *et al.*

However, if our Yarkovsky removal rate function were several times stronger or weaker, we would see a mismatch in not only in the observed number of NEOs but also in the number of main belt objects.

The interesting element here is that the small kink observed in the NEO population near $D \sim 0.7$ km is apparently real; note that our Yarkovsky/resonance removal rate function has no inflection points in that size range. A reasonable explanation for the kink is that it is produced by the Yarkovsky effect, which samples $D \lesssim 30$ km bodies from across the wave-shape main belt size distribution and delivers them to resonances. Thus, the kink provides additional evidence that most NEOs come from the main belt and that the Yarkovsky effect is the dominant physical process providing asteroids to resonances.

6. The Evolution of Asteroid Families and Stony Meteoroids

Now that we have a reasonably accurate model of how the main belt and NEO size distributions evolved over solar system history, we can return to the issue of stony meteoroid production, evolution, and delivery to the Earth. For the moment, we concentrate on what happens to main belt meteoroids produced by a single homogeneous and distinct parent body.

A cratering or catastrophic disruption event on our parent body will produce a fragment size distribution (FSD); we assume the event in question is large enough that the FSD includes both meter-sized bodies (meteoroids) as well as larger objects. Subsequent collisions onto bodies in the FSD act as a source for new meteoroids that are genetically the same as those created in the previous generation. This so-called collisional cascade guarantees that meteoroids from this parent body will be provided to the main belt

population (and possibly to Earth) for some time after the initial impact event (e.g., Williams & Wetherill 1994). At the same time, dynamical processes and collisions onto the newly-created meteoroids act as a sink to eliminate them from the main belt. Thus, after the initial collision event, the sources and sinks drive the meteoroid population toward a quasi-steady state. If the sinks dominate the sources, the meteoroid population will undergo a slow (or not so slow) decay as collisions on the FSD deplete the reservoir of larger bodies capable of replacing them. The size and nature of this reservoir, therefore, determine the decay rate of the meteoroid population.

To simulate this process, we modified CoDDEM to track input FSDs evolving within the main belt population. We then tested how FSDs produced by parent bodies having the same diameter as the central body in each bin of our size distribution (e.g., $D = 31, 39, 47, 61, 77, 98, 123, 155, \dots$) would react to collisions and dynamical depletion via the Yarkovsky effect/resonances over main belt history. We also assumed the collision probability between family members was the same as family members with the background population. This is an oversimplification of reality but reasonable given the approximations used in this work.

Our chief unknown was the nature of the FSD used in each simulation. Note that numerical hydrocode results and observations of asteroid families indicate that FSDs produced by cratering or disruption events can be very different from one another, with factors like impact energy, parent body size, impact angle, etc. playing critical roles in the outcome (e.g., Tanga *et al.* 1999; Michel 2001; 2002; 2003; Durda *et al.* 2004). For this reason, we decided to create a “toy” FSD for each body that was purposely exaggerated to test the extremes of the problem (and one that is inconsistent with the FSDs described previously). Our goal here was not to concentrate on absolute numbers delivered to Earth but instead to compute an approximate decay rate for the meteoroid population produced by each toy FSD. The criteria used to create our toy FSDs were as follows:

- (i) the FSD had to have the same mass as the parent body when computed over the size intervals with $D > 0.001$ km,
- (ii) the FSD had to follow a single power law slope, though that slope could be different for different parent body sizes
- (iii) the number of meteoroids in the FSD had to be a factor of ~ 2 smaller than the number of meteoroids in the main belt population.

Accordingly, the breakup of our parent object would produce a FSD that would immediately dominate the main belt meteoroid population. This is not as absurd as it seems at face value; CoDDEM results predict the main belt contains $\sim 10^{12}$ meter-sized objects, which is only the mass equivalent of a single 10-20 km asteroid. Still, this estimate likely overestimates the number of meteoroids produced by small families. The reason we use it is that it places all our toy FSDs on the same initial footing. If smaller asteroid disruption events fail to dominate the meteoroid population under an exaggerated situation, they are similarly unlikely to dominate under more realistic conditions.

Fig. 3 shows the what happens when FSDs produced by $D = 30$ km and 100 km parent bodies are placed in the main belt ~ 3.1 Ga (1.5 Gy after solar system formation). We made sure this time took place after the LHB, whose effects on the main belt population may have been important. For the FSD derived from the 30 km body, we find that the initial meteoroid population (i.e., meter-sized bodies) drops by a factor of 100 and 10^5 within 130 My and 3.1 Gy, respectively (Fig. 4). Thus, FSDs produced by < 30 km

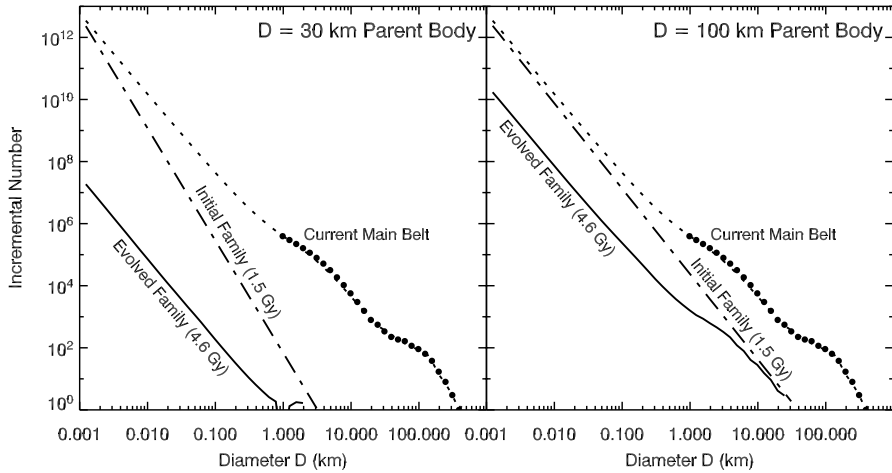


Figure 3. The collisional and dynamical evolution of two “toy” asteroid families produced by the disruption of a $D = 30$ and 100 km parent bodies. Both families were inserted into CoDDEM at 1.5 Gy after solar system formation. The meteoroid population is represented by the number of bodies in the $D \sim 0.001$ km size bin. The solid lines show the families at present (4.6 Gy). The smaller family has decayed significantly more than the larger family. Note the shallow slope of the $D = 100$ km family for $0.7 \lesssim D \lesssim 5$ km. This shape mimics the that of the background main belt population over the same size range. Morbidelli *et al.* (2003) found the same kinds of shallow slopes in many prominent asteroid families. This suggests these families are old enough to have experienced significant comminution.

parent bodies decay away so quickly that ancient ones are unlikely to deliver meaningful numbers of meteoroids to Earth today. For the 100 km parent body, the decay rate is significantly slower, with the meteoroid population only dropping by a factor of 100 over $2\text{--}3$ Gy. This suggests that many meteoroids reaching Earth today come from prominent asteroid families with sizable FSDs, even if those families were created billions of years ago.

Another interesting aspect of the evolution of the 100 km parent body’s FSD is that comminution produces a shallow slope between $0.7 \lesssim D \lesssim 5$ km. We note that shallow slopes in this size range have been observed among the FSD of many prominent asteroid families (Morbidelli *et al.* 2003). Our simulations suggest this slope is produced by collisional evolution and is a function of several factors: the “V”-shaped Q_D^* function used by CoDDEM (e.g., Benz & Asphaug 1999; Bottke *et al.* 2004a), the number of $D \gtrsim 10$ km objects in the FSD, and the bombardment of the FSD from the background main belt population. As the FSD evolves via collisions and dynamical depletion, smaller objects are eliminated faster than they can be replenished by disruption events among bigger objects. Conversely, $D > 10$ km objects in the FSD (and in the main belt) are hard to disrupt, partly because these bodies have relatively high Q_D^* values but also because the main belt population’s wavy shape provides relatively few projectiles capable of disrupting $D > 10$ km targets. This means that objects moderately smaller than $D \sim 10$ km are not replenished very often. The net result is that (i) the smallest objects in the FSD become depleted and evolve to the same slope as the background main belt population

(e.g., O'Brien & Greenberg 2003), (ii) the $D > 10$ km population undergoes few changes, and (iii) the $0.7 \lesssim D \lesssim 5$ km objects evolve to a shallow slope that connects these two extremes, producing a shallow slope reminiscent of the slope of the main belt population in the same size range. In some test cases, we even find the slope in (iii) can be more shallow than the background population, a result consistent with some observed families (Morbidelli *et al.* 2003).

In order to compute a rough measure of how many stony meteorites should be in our collection, we combined the meteoroid decay rates taken from the evolution of our toy FSDs with CODDEM estimates of the production rates of asteroid families over the last ~ 4 Gy. We attempted to keep things as simple as possible for this calculation by assuming the following: (i) meteoroids from all parts of the main belt have an equal chance of reaching Earth, (ii) all $D > 30$ km asteroids disrupted over the last several Gy have the capability of producing a distinct class of meteorites, and (iii) once a family's meteoroid production rate drops by a factor of 100, it is unlikely to produce enough terrestrial meteorites to be noticed in our collection. The latter choice is somewhat arbitrary, but it is meant to partially balance against the possibility that our FSDs are too steep for smaller parent bodies.

Our CoDDEM results suggest that asteroid families produced by the breakup of $D \gtrsim 100$ km bodies have such slow meteoroid decay rates that all ~ 20 of them may very well be providing meteoroids today, regardless of their disruption time over the last 3-4 Gy. While this is a substantial number, it is not enough to explain the diversity of stony meteorites observed in our collection. Moreover, Nesvorný *et al.* (2004) estimate that only $\sim 40\%$ of the main belt down to a few km in diameter is comprised of asteroids from the largest families.

Among the smaller parent bodies ($30 < D < 100$ km), we find that, on average, the interval between disruption events across the main belt is short enough that many have disrupted over the last Gy or so (e.g., CoDDEM results predict a $D \sim 30$ km body disrupts once every 25 My; a $D \sim 80$ km body disrupts once every 160 My). We combine these numbers with our meteoroid decay rate values to estimate the number of parent bodies producing distinct classes of meteorites. For example, Fig. 4 shows that the meteoroid population produced by $D \sim 30$ km bodies decays by a factor of 100 over 130 My. This means that if our toy FSD is reasonable, ~ 5 stony meteorite classes ($130 \text{ My} / 25 \text{ My}$) should come from families produced by the breakup of these size bodies. Making comparable calculations for disruption events among $30 < D < 100$ km bodies, we estimate that we should see meteorites from another ~ 25 parent bodies.

Summing our values, we estimate we should find stony meteorites from ~ 45 different parent bodies. The actual value is ~ 30 parent bodies. We consider this to be surprisingly good match when all of our model uncertainties are considered. It also implies that some breakup events occurred recently enough that their FSDs at small sizes may still have power law slopes steeper than the background population.

Other than model inaccuracies, we believe there are several plausible reasons why our estimates come out 50% higher than the observed value. Two important ones are listed here:

1. Some disruption events must occur within existing families. A prominent example would be the Karin cluster, which was produced by the breakup of a $D \sim 25$ -30 km asteroid inside the Koronis asteroid family (Nesvorný *et al.* 2002; 2003; Nesvorný & Bottke 2004). Because intra-family breakups are unlikely to produce distinct classes of stony meteoroids, this would decrease the total number of parent bodies represented in our model.

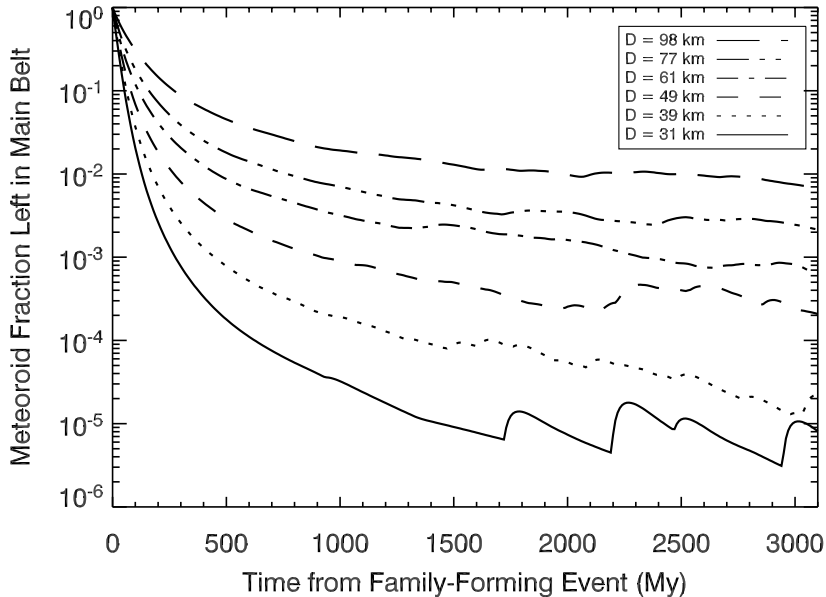


Figure 4. Decay rates of meteoroid populations from our “toy” asteroid families produced from parent bodies with $30 < D < 100$ km. All families were inserted in CoDDEM at 1.5 Gy after solar system formation. The smallest families decrease by a factor of 100 over a few 0.1 Gy while the largest take several Gy to decay by the same value.

2. Outer main belt meteoroids may have great difficulty reaching Earth. For example, Morbidelli & Gladman (1998) have shown that bodies from the ν_6 secular resonance (along the inner edge of the main belt from 2.1–2.5 AU) have a $\sim 1\%$ chance of striking the Earth, while those from the 5:2 resonance at 2.8 AU only have a $\sim 10^{-5}$ chance. The latter probability is low because most bodies placed in the 5:2 resonance readily reach Jupiter-crossing orbits, a characteristic shared by most outer main belt resonances. Moreover, many outer main belt meteoroids may also be analogous to weak carbonaceous chondritic material, which would make their survival through our atmosphere problematic. Taken together, these factors suggest that only the most prolific meteoroid producers in the outer main belt produce meteorites.

We believe these factors could reduce the number of sampled parent bodies in our model enough to match observations. To prove it, we will need to develop a next-generation meteoroid evolution model that accounts for the coupled collisional/dynamical evolution of families as they stretch toward main belt resonances (e.g., Morbidelli & Vokrouhlický 2003). This model will also need to include more realistic FSD estimates than those used here.

Before concluding, we have one additional observation to make about our results. Constraints that can be used to test our model include various meteorite CRE age distributions (e.g., H, L, and LL chondrites; Marti & Graf 1992; Morbidelli & Gladman 1998; Vokrouhlický & Farinella 2000; Eugster 2003). Our model implies that the wide range of CRE ages observed among the H, L, and LL meteorite classes (~ 10 –100 My) are unlikely to come from multiple cratering events on a single parent body (e.g., Migliorini *et al.* 1997). Instead, we postulate they come from small-scale (or not so small-scale) breakup

events occurring among family members, where the family itself might stretch from its point of origin all the way to multiple resonant routes leading to Earth. In this scenario, concentrations of CRE ages among meteorite classes, such as the $\sim 7\text{-}8$ Ma cluster measured on almost half of the H chondrites (Eugster 2003), would come from distinct breakups events occurring near the resonances. The quantity of meteorites within a given CRE age cluster would then depend on the size of the disrupted immediate precursor, its proximity to the resonance, and the likelihood that material in that resonance would reach Earth.

7. Conclusions

Our main belt evolution model provides results that are consistent with the limited number of parent bodies represented in our stony meteorite collection. We believe that most stony meteorites are byproducts of a collisional cascade, with some coming from asteroid families produced by the breakup of $D > 100$ km bodies over the last several Gy and the remainder coming from smaller, more recent breakup events among $D < 100$ km asteroids that occurred over recent times (i.e., $\ll 1$ Gy).

Other notable results described in the paper include the following: (i) the wavy main belt size distribution is likely a “fossil” produced by collisions taking place in the first few tens of My of solar system history; (ii) the kink in the NEO size distribution near $D \sim 0.7$ km is likely a by-product of the Yarkovsky effect/resonances working on the wavy main belt population, and (iii) collisional evolution likely explains why so many observed asteroid families have shallow power law slopes in the size interval $0.7 < D < 5$ km (Morbidelli *et al.* 2003).

Acknowledgements

We thank Dave O’Brien for valuable discussions and input to this study. We also thank Kleomenis Tsiganis for his careful and useful review of this paper. Research funds for William Bottke were provided by NASA’s Origins of Solar Systems (grant NAG5-10658) and Planetary Geology and Geophysics Programs (grant NAG5-13195).

References

- Agnor, C.B., Canup, R.M. & Levison, H.F. 1999, *Icarus* 142, 219
- Asphaug, E., Ryan, E.V. & Zuber, M.T. 2002, in: Bottke, W.F., Cellino, A., Paolicchi, P. & Binzel, R.P. (eds.), *Asteroids III* (Univ. Arizona Press, Tucson), p. 463.
- Benz, W. & Asphaug, E. 1999, *Icarus* 142, 5
- Bland, P.A., Conway, A., Smith, T.B., Berry, F.J. & Pillinger, C.T. 2000, in: Grady M. M., Hutchison R., McCall G. J. H. & Rothery D. A. (eds) *Meteorites: Flux with Time and Impact Effects*. Geological Society, London, Special Publications 140, p.43
- Bottke, W.F. & Greenberg, R. 1993, *Geophys. Res. Lett.* 20, 879
- Bottke, W.F., Nolan, M.C., Greenberg, R. & Kolvoord, R.A. 1994, *Icarus* 107, 255.
- Bottke, W.F., Rubincam, D.P. & Burns, J.A. 2000, *Icarus* 145, 301
- Bottke, W.F., Jedicke, R., Morbidelli, A., Petit, J.-M. & Gladman, B.J. 2000, *Science* 288, 2190

- Bottke, W.F., Vokrouhlický, D., Brož, M., Nesvorný, D. & Morbidelli, A. 2001, *Science* 294, 1693
- Bottke, W.F., Morbidelli, A., Jedicke, R., Petit, J.-M., Levison, H.F., Michel, P. & Metcalfe, T.S. 2002a, *Icarus* 156, 399
- Bottke, W.F., Vokrouhlický, D., Rubincam, D.P. & Brož, M. 2002b, in: Bottke, W.F., Cellino, A., Paolicchi, P. & Binzel, R.P. (eds.), *Asteroids III* (The University of Arizona Press, Tucson), p. 395
- Bottke, W. F., Durda, D.D., Nesvorný, D., Jedicke, R. Morbidelli, A., Vokrouhlický, D. & Levison., H.L. 2004a. *Icarus*, in press
- Bottke, W. F., Durda, D.D., Nesvorný, D., Jedicke, R. Morbidelli, A., Vokrouhlický, D. & Levison., H.L. 2004b. *Icarus*, in preparation
- Britt, D.T., Yeomans, D., Housen, K., Consolmagno, G. 2002, in: Bottke, W.F., Cellino, A., Paolicchi, P. & Binzel, R.P. (eds.), *Asteroids III* (Univ. Arizona Press, Tucson), p. 485
- Burbine, T.H., McCoy, T.J., Meibom, A., Gladman, B. & Keil, K. 2002, in: Bottke, W.F., Cellino, A., Paolicchi, P. & Binzel, R.P. (eds.), *Asteroids III* (Univ. Arizona Press, Tucson), p. 653
- Campo Bagatin, A., Cellino, A., Davis, D.R., Farinella, P. & Paolicchi, P. 1994, *Planet. Space Sci.* 42, 1079
- Caffee, M.W., Reedy, R.C., Goswami, J.N., Hohenberg, C.M. & Marti, K. 1988, in: Kerridge, J.F. & Matthews, M.S. (eds.), *Meteorites and the Early Solar System* (Univ. Arizona Press, Tucson), p. 205.
- Chambers, J.E. & Migliorini, F. 1997, *Bull. Amer. Astron. Soc.* 29, 1024
- Chambers, J.E. & Wetherill, G.W. 1998, *Icarus* 136, 304
- Chambers, J.E. & Wetherill, G.W. 2001, *Meteoritics Planet. Sci.* 36, 381.
- Davis, D.R., Durda, D.D., Marzari, F., Campo Bagatin, A. & Gil-Hutton, R. 2002, in: Bottke, W.F., Cellino, A., Paolicchi, P. & Binzel, R.P. (eds.), *Asteroids III* (Univ. Arizona Press, Tucson), p. 545
- Dohnanyi, J.W. 1969, *J. Geophys. Res.* 74, 2531
- Durda, D.D., Greenberg, R. & Jedicke, R. 1998, *Icarus* 135, 431
- Durda, D.D., Bottke, W.F., Enke, B.L., Merline, W.J., Asphaug, E., Richardson, D.C., & Leinhardt, Z.M. 2004, *Icarus* 170, 243
- Eugster, O. 2003, *Chemie der Erde* 63, 3
- Farinella, P. & Davis, D.R. 1992, *Icarus* 97, 111
- Farinella, P., Froeschlé, Ch, Froeschlé, Cl., Gonczi, R., Hahn, G., Morbidelli, A. & Valsecchi, G.B. 1994. *Nature* 371, 315
- Farinella, P. & Vokrouhlický, D. 1999, *Science* 283, 1507
- Farinella, P., Vokrouhlický, D. & Hartmann, W.K. 1998, *Icarus* 132, 378
- Fowler, J.W. & Chillemi, J.R. 1992, in: E.F. Tedesco, (ed) *The IRAS Minor Planet Survey* (Tech. Report PL-TR-92-2049., Phillips Laboratory, Hanscom Air Force Base, Massachusetts) p. 17
- Gomes, R., Morbidelli, A., Tsiganis, K., & Levison, H. 2004, *AAS/Division for Planetary Sciences Meeting* 36, 1167
- Grieve, R. A. F. & Shoemaker, E. M. 1994, in: Gehrels, T. & Matthews, M.S. (eds.) *Hazards Due to Comets and Asteroids* (Univ. Arizona Press, Tucson) p. 417
- Guillot, T., Hueso, R. 2003, *Bull. Amer. Astron. Soc.* 35
- Gladman, B.J., Migliorini, F., Morbidelli, A., Zappalà, V., Michel, P., Cellino, A., Froeschlé, C., Levison, H.F., Bailey, M. & Duncan, M. 1997, *Science* 277, 197
- Grady, M. *Catalogue of meteorites* (U. Cambridge Press).
- Greenberg, R. 1982, *Astron. J.* 87, 184
- Hartmann, W. K., Ryder, G., Dones, L. & Grinspoon, D. 2000, in: Canup, R. & Righter, K., (eds.) *Origin of the Earth and the Moon* (Univ. Arizona Press, Tucson) p. 805
- Holsapple, K., Giblin, I., Housen, K., Nakamura, A. & Ryan, E. 2002, in: Bottke, W.F., Cellino, A., Paolicchi, P. & Binzel, R.P. (eds.), *Asteroids III* (Univ. Arizona Press, Tucson), p. 443.

- Inaba, S., Wetherill, G.W. & Ikoma, M. 2003, *Icarus* 166, 46
- Ivezić, Z. & 31 coauthors 2001, *Astron. J.* 122, 2749
- Jedicke, R., Larsen, J. & Spahr, T. 2002, in: Bottke, W.F., Cellino, A., Paolicchi, P. & Binzel, R.P. (eds.), *Asteroids III* (Univ. Arizona Press, Tucson), p. 71.
- Keil, K. 2002, *Planet. Space Sci.* 48, 887.
- Keil, K. 2002, in: Bottke, W.F., Cellino, A., Paolicchi, P. & Binzel, R.P. (eds.), *Asteroids III* (Univ. Arizona Press, Tucson), p. 573.
- Levison, H.F. & Duncan, M.J. 1994, *Icarus* 108, 18
- Love, S.G. & Ahrens, T.J. 1997, *Nature* 386, 154
- Marti, K. & Graf, T. 1992, *Ann. Rev. Earth Planet. Sci.* 20, 221
- Meibom A. & Clark, B.E. 1999, *Meteoritics Planet. Sci.* 34, 7.
- Michel, P., Benz, W., Tanga, P. & Richardson, D. 2001, *Science* 294, 1696.
- Michel, P., Tanga, P., Benz, W. & Richardson, D. 2002, *Icarus* 160, 10
- Michel, P., Benz, W. & Richardson, D. 2003, *Nature* 421, 608
- Morbidelli, A. & Gladman, B. 1998, *Meteoritics Planet. Sci.* 33, 999
- Morbidelli, A., Petit, J.-M., Gladman, B. & Chambers, J. 2001, *Meteoritics Planet. Sci.* 36, 371
- Morbidelli, A., Nesvorný, D., Bottke, W.F., Michel, P., Vokrouhlický, D. & Tanga, P. 2003, *Icarus* 162, 328.
- Morbidelli, A. & Vokrouhlický, D. 2003, *Icarus* 163, 120
- Nesvorný, D. & Bottke, W.F. 2004, *Icarus* 170, 324
- Nesvorný, D., Bottke, W.F., Dones, L. & Levison, H.F. 2002, *Nature* 417, 720
- Nesvorný, D., Bottke, W.F., Levison, H.F. & Dones, L. 2003, *Astrophys. J.* 591, 486
- Nesvorný, D. & Bottke, W.F. 2004, *Icarus* 170, 324
- Nesvorný, D., Jedicke, R., Whiteley, R.J. & Ivezić, Ž 2004, *Icarus*, in press.
- O'Brien, D.P. & Greenberg, R. 2003, *Icarus* 164, 334
- Öpik, E.J. 1951, *Proc. R. Irish Acad.* 54, 165.
- Petit, J., Morbidelli, A. & Valsecchi, G.B. 1999, *Icarus* 141, 367.
- Petit, J., Morbidelli, A. & Chambers, J. 2001, *Icarus* 153, 338
- Petit, J.-M., Chambers, J., Franklin, F. & Nagazawa, M. 2002, in: Bottke, W.F., Cellino, A., Paolicchi, P. & Binzel, R.P. (eds.), *Asteroids III* (Univ. Arizona Press, Tucson), p. 711.
- Pollack, J.B., Hubickyj, O., Bodenheimer, P., Lissauer, J., Podolak, M. & Greenzweig, Y. 1996, *Icarus* 124, 62.
- Press, W.H., Flannery, B.P., Teukolsky, S.A. & Vetterling, W.T. 1989, *Numerical recipes in Fortran. The art of scientific computing* (Cambridge: University Press)
- Rubincam, D. P. 2000, *Icarus* 148, 2
- Stuart, J.S. & Binzel, R.P. 2004, *Icarus* 170, 295
- Stokes, G.H., Yeomans, D.K., Bottke, W.F., Chesley, S.R., Evans, J.B., Gold, R.E., Harris, A.W., Jewitt, D., Kelso, T.S., McMillan, R.S., Spahr, T.B. & Worden, S.P. 2003, *Report of the Near-Earth Object Science Definition Team: A Study to Determine the Feasibility of Extending the Search for Near-Earth Objects to Smaller Limiting Diameters*. NASA-OSS-Solar System Exploration Division.
- Tanga, P., Cellino, A., Michel, P., Zappalà, V., Paolicchi, P. & Dell'Oro, A. 1999, *Icarus* 141, 65
- Tedesco, E.F. & Desert, F. 2002, *Astron. J.* 123, 2070
- Tedesco, E.F., Noah, P.V., Noah, M. & Price, S.D. 2002, *Astron. J.* 123, 1056
- Tsiganis, K., Morbidelli, A., Levison, H. F. & Gomes, R. S. 2004, *AAS/Division of Dynamical Astronomy Meeting* 35, 1177.
- Vokrouhlický, D. & Farinella, P. 2000, *Nature* 407, 606
- Weidenschilling, S.J. 1977, *Astrophys. Space Sci.* 51, 153
- Wetherill, G.W. 1989, 2002, in: Binzel, R.P., Gehrels, T. & Matthews, M.S. (eds.), *Asteroids II* (Univ. Arizona Press, Tucson), p. 661.

- Wetherill, G.W. 1967, *J. Geophys. Res.* 72, 2429.
- Wetherill, G.W. & Stewart, G.R. 1989, *Icarus* 77, 330
- Williams, D.R. & Wetherill, G.W. 1994., *Icarus* 107, 117
- Wuchterl, G., Guillot, T. & Lissauer, J.J. 2000, in: Manning, V., Boss, A.P. & Russell, S.S. (eds.), *Protostars and Planets IV* (Univ. Arizona Press, Tucson), p. 1081
- Zappalà, V., Cellino, A., dell'Oro, A. & Paolicchi, P. 2002, in: Bottke, W.F., Cellino, A., Paolicchi, P. & Binzel, R.P. (eds.), *Asteroids III* (The Univ. Arizona Press, Tucson), p. 619.